Preprints of the 21st IFAC World Congress (Virtual)
Berlin, Germany, July 12-17, 2020

Control Lyapunov Function Based Finite-Horizon Optimal Control for Repointing of a Spacecraft ⋆

Yuanzhuo Geng * **Chuanjiang Li** * **Yanning Guo** *
James Douglas Biggs **

* *Department of Control Science and Engineering, Harbin Institute of Technology, Harbin, 150001, China(e-mail:gengyz@hit.edu.cn)*
** *Polytechnic University of Milan, 20156 Milan, Italy (e-mail: jamesdouglas.biggs@polimi.it)*

Abstract: This paper addresses the problem of optimally repointing the optical axis of a spacecraft to align with the target direction. A new metric defining the repointing error is proposed where the corresponding kinematic equations provide a simple and convenient form for control design. The proposed control integrates a Control Lyapunov Function (CLF) approach with a sliding mode controller which simultaneously guarantees the optimality and robustness of the closed-loop system. Firstly, a CLF based control scheme is used to ensure that the state optimally converges to the sliding surface. Then a fixed-time non-singular terminal sliding mode controller is employed to provide robust convergence to the origin along the sliding surface. The convergence time is finite for any initial states and is thus useful for applications with critical time constraints. The region of attraction and convergence time is analyzed. Finally, numerical investigations are conducted to verify the effectiveness and superiority of the proposed algorithm with respect to the classical CLF method.

Keywords: Repointing maneuver; Nonlinear optimal control; Control Lyapunov function; Fixed-time sliding mode control

1. INTRODUCTION

Space-based observation requires precision pointing, where the spacecraft should point to (stare at) the target for a prescribed period of time. In some applications, such as the GF-4 satellite for weather monitoring, Jilin-1 video satellite for remote sensing, and LAPAN-Tubsat for Earth observation, control of the optical axis is not required, and the attitude control problem can be reduced, enabling more freedom and flexibility for control design and optimization.

The attitude modeling and control for spacecraft operating in staring-mode has been investigated in (Lian et al. (2017); Pong and Miller (2015); Hu et al. (2018b)). In these papers, the target direction is described by an elevation angle and an azimuth angle. However, the corresponding repointing error kinematics are overly complex and the representation used is ambiguous. A simple and practical description for the error of repointing maneuvers is presented here. This new error metric and error kinematics provide a convenient form for an optimal control to be derived that drives the trajectory onto a sliding surface.

In this paper we design the control to minimize an infinite-time integral cost function of the state error and control torques. To solve linear optimal control problems, the Linear Quadratic Riccati (LQR) method, and the State-Dependent Riccati Equation (SDRE) method (see Geng et al. (2019)) have been proposed. However, spacecraft kinematics cannot be approximated accurately using linearized dynamics for large-angle maneuvers or for large angular rates , thus the LQR and the SDRE method will not provide optimal performance.

A Control Lyapunov Function(CLF) based control synthesis was proposed by Primbs (Primbs et al. (1999)) as a tool for nonlinear optimal control design. The CLF links optimal control with Lyapunov stability theory. Moreover, the approach here constructs a CLF where the gradient of the optimal value function(cost-to-go function) $\partial V^*/\partial \boldsymbol{x}$ is replaced with the gradient of a CLF multiplied by a state-dependent scalar, namely $\lambda(\boldsymbol{x})\partial V^*/\partial \boldsymbol{x}$. This method yields a stable suboptimal controller that is much simpler to implement than more traditional nonlinear optimal control methods. Moreover, this optimal control approach does not involve the complex task of solving the HJB equations (see Park (2005); Haddad and L'Aitto (2015)). This control formulation is intrinsically a gain-scheduling PD control where the time-varying gains are used to enhance optimality. However, note that the control approach is only sub-optimal in that it is optimal only for the case that $\partial V^*/\partial \boldsymbol{x}$ and $\partial V/\partial \boldsymbol{x}$ are in the same direction.

In addition, the CLF method is sensitive to external disturbances. Moreover there is no active mechanism in CLF control for disturbance suppression, and it only guaran-

⋆ This work is supported by China Scholarship Council, the National Natural Science Foundation of China (Grants No. 61876050, 61973100 and 61673135).

tees robustness passively. Therefore the control performance of CLF methods degrades significantly when the system is affected by disturbances. In contrast, sliding mode control(SMC) is well known for its good robustness properties. Recently, finite-time and fixed-time terminal sliding mode controls have been extensively studied where the state converges to the origin in finite time (Hu et al. (2017a,b, 2018a); Corradini and Cristofaro (2018); Zuo (2014, 2015); Wang et al. (2009)). Ensuring the robustness of spacecraft pointing is critical for precise imaging and observation in the presence of external disturbances due to solar radiation pressure, air drag and magnetic effects.

In this paper, our goal is two-fold: firstly, a simple representation for the repointing error and the corresponding attitude error kinematics is presented. Secondly, a two-phase sliding mode based CLF scheme(TSCLF) is proposed. This approach guarantees the optimality of the system while enhancing the robustness of the classical CLF method. Moreover it links the finite-time control with optimal control.

The paper is organized as follows. In Section 2, preliminaries for CLF control design are introduced. Then the repointing attitude kinematics are derived in Section 3. The main result is established in Section 4 where the two-phase CLF suboptimal control approach is investigated for repointing maneuvers. An illustrative numerical example and simulation comparisons are presented in Section 5.

2. MATHEMATICAL PRELIMINARIES

Consider the following affine nonlinear system

$$\dot{\boldsymbol{x}} = \boldsymbol{f}(\boldsymbol{x}) + \boldsymbol{g}(\boldsymbol{x})\boldsymbol{u} \tag{1}$$

with a performance index J to be minimized which is defined by

$$J = \int_0^\infty (l(\boldsymbol{x}) + \boldsymbol{u}^{\mathrm{T}}\boldsymbol{R}\boldsymbol{u})dt \tag{2}$$

where $\boldsymbol{x} \in R^n$ and $\boldsymbol{u} \in R^m$ are the state and control variables respectively, $\boldsymbol{f} : R^n \to R^n$ and $\boldsymbol{g} : R^n \to R^m$ are vector and matrix-valued functions with $\boldsymbol{f}(\boldsymbol{0}) = \boldsymbol{0}$. The state-related function $l(\boldsymbol{x})$ is a positive definite function, $\boldsymbol{R} \in R^{m\times m}$ is positive definite.

Let $V(\boldsymbol{x})$ be a Lyapunov function for the system of (1) and its derivative is given by

$$\dot{V} = L_f V + L_g V \boldsymbol{u} \tag{3}$$

where L represents the Lie derivative operator, $L_f V = \frac{\partial V^{\mathrm{T}}}{\partial \boldsymbol{x}}\boldsymbol{f}$, $L_g V = \frac{\partial V^{\mathrm{T}}}{\partial \boldsymbol{x}}\boldsymbol{g}$.

Now, $V(\boldsymbol{x})$ is a CLF (Sontag (1989)) if $\forall \boldsymbol{x} \neq \boldsymbol{0}$,

$$L_g V = \boldsymbol{0} \Rightarrow L_f V < 0 \tag{4}$$

For nonlinear optimal control, the most intractable issue is to solve the HJB equation

$$l(\boldsymbol{x}) + L_f V^* - \frac{1}{4}(L_g V^*)\boldsymbol{R}^{-1}(L_g V^*)^{\mathrm{T}} = 0 \tag{5}$$

where $V^*(\boldsymbol{x})$ is the state-dependent optimal value function (cost-to-go) to be solved which is defined as

$$V^*(\boldsymbol{x}) = \inf_{\boldsymbol{u}} \int_t^\infty (l(\boldsymbol{x}) + \boldsymbol{u}^{\mathrm{T}}\boldsymbol{R}\boldsymbol{u})dt \tag{6}$$

If there exists a continuously differentiable, positive definite solution of the HJB equation of (5), then the optimal control is derived based on Pontryagin's minimum principle as

$$\boldsymbol{u}^* = -\frac{1}{2}\boldsymbol{R}^{-1}(L_g V^*)^{\mathrm{T}} \tag{7}$$

An alternate approach to optimal control comes from the Sontag's formula(Sontag (1989)), in essence, uses the directional information supplied by a CLF, V, and scales it properly to solve the HJB equation. Assuming the relationship between V^* and V can be defined as $\partial V^*/\partial \boldsymbol{x} = \lambda(\boldsymbol{x})\partial V/\partial \boldsymbol{x}$, where $\lambda(\boldsymbol{x})$ is a scalar function. Then the optimal controller of (7) is

$$\boldsymbol{u}^* = -\frac{1}{2}\boldsymbol{R}^{-1}\lambda(\boldsymbol{x})(L_g V)^{\mathrm{T}} \tag{8}$$

By substituting $L_g V^* = \lambda(\boldsymbol{x})L_g V$ and $L_f V^* = \lambda(\boldsymbol{x})L_f V$ into the HJB equation of (5), it can be derived that

$$l(\boldsymbol{x}) + \lambda L_f V - \frac{\lambda^2}{4}(L_g V)\boldsymbol{R}^{-1}(L_g V)^{\mathrm{T}} = 0 \tag{9}$$

from which $\lambda(\boldsymbol{x})$ can be solved with the predefined CLF V as

$$\lambda(\boldsymbol{x}) = 2\frac{L_f V + \sqrt{(L_f V)^2 + l(\boldsymbol{x})(L_g V)\boldsymbol{R}^{-1}(L_g V)^{\mathrm{T}}}}{(L_g V)\boldsymbol{R}^{-1}(L_g V)^{\mathrm{T}}} \tag{10}$$

Substituting the value of $\lambda(\boldsymbol{x})$ to (8), the control input $\boldsymbol{u}^*$ is expressed as

$$\boldsymbol{u}^* = \begin{cases} -\boldsymbol{R}^{-1}\left[\dfrac{a + \sqrt{a^2 + l(\boldsymbol{x})\boldsymbol{b}\boldsymbol{R}^{-1}\boldsymbol{b}^{\mathrm{T}}}}{\boldsymbol{b}\boldsymbol{R}^{-1}\boldsymbol{b}^{\mathrm{T}}}\right]\boldsymbol{b}^{\mathrm{T}}, & \text{if } \boldsymbol{b} \neq \boldsymbol{0} \\ \boldsymbol{0} & \text{else} \end{cases} \tag{11}$$

where $a = L_f V$, $\boldsymbol{b} = L_g V$.

The performance index defined in (2) contains the control effort and state errors. Note that the control law in (11) is just suboptimal instead of truly optimal because the assumption of $\partial V^*/\partial \boldsymbol{x} = \lambda(\boldsymbol{x})\partial V/\partial \boldsymbol{x}$ limits the gradient direction of V^* with respect to $\boldsymbol{x}$. Besides, the real optimal cost-to-go function V^* satisfies the HJB equation completely but $\lambda(\boldsymbol{x})V_x$ only satisfies the HJB equation in the case of $L_g V \neq \boldsymbol{0}$.

3. ATTITUDE MODEL OF A SPACECRAFT OPERATING IN STARING-MODE

3.1 Attitude motion of spacecraft

The rotational dynamics of a rigid spacecraft are described as

$$\dot{\boldsymbol{\omega}}_{bi} = -\boldsymbol{J}_{\mathrm{s}}^{-1}\boldsymbol{\omega}_{bi}^{\times}\boldsymbol{J}_{\mathrm{s}}\boldsymbol{\omega}_{bi} + \boldsymbol{J}_{\mathrm{s}}^{-1}(\boldsymbol{u} + \boldsymbol{d}) \tag{12}$$

where $\boldsymbol{\omega}_{bi}$ is the angular velocities vector with respect to the inertial frame expressed in the body frame, $\boldsymbol{u}$

represents the control torque, $\boldsymbol{J}_{\mathrm{s}}$ is the inertia matrix, $\boldsymbol{d}$ denotes disturbance torque. We use $\boldsymbol{a}^{\times}$ to denote the skew-symmetric matrix of $\boldsymbol{a} = [a_1\ a_2\ a_3]^{\mathrm{T}}$.

3.2 Novel definitions for repointing errors

Euler angles are always employed to describe the repointing attitude of staring-mode spacecraft, but they are complicated and the corresponding kinematics may be singular in the case of large angle maneuvers. In this paper, a new representation is used that is convenient for the optimal control law design. In the following description, the superscript $(\cdot)^i$, $(\cdot)^b$ represents that the vector is expressed in the inertial frame and body fixed frame respectively.

Assume that the optical payload is fixed along the X_b axis of the spacecraft. Define the error variables as follows:

$$\begin{aligned} &\boldsymbol{e} = [e_x\ e_y\ e_z]^{\mathrm{T}} = \boldsymbol{C}_{bi}\boldsymbol{t}^i - [1\ 0\ 0]^{\mathrm{T}} \\ &e_x = \cos\theta_x - 1, e_y = \cos\theta_y, e_z = \cos\theta_z \end{aligned} \tag{13}$$

where θ_x, θ_y, and θ_z denotes the angle between the three body axis and the target direction $\boldsymbol{t}$ whose desired value are $\theta_{xd} = 0$, $\theta_{yd} = \frac{\pi}{2}$, $\theta_{zd} = \frac{\pi}{2}$. $\boldsymbol{C}_{bi}$ is direction-cosine matrix between the body frame and the inertial frame.

3.3 Pointing error kinematics and dynamics of a staring mode spacecraft for space target observation

For some space observation missions, such as Moon observation, and Mars detection, the targets are very far from the spacecraft. Thus for simplicity of exposition, the orbit motion of the spacecraft in an Earth orbit can be omitted when calculating the desired pointing directions.

The pointing error dynamics can be obtained from (12) and (13) as

$$\begin{aligned} \dot{\boldsymbol{e}} &= \dot{\boldsymbol{C}}_{bi}\boldsymbol{t}^i = \boldsymbol{F}\boldsymbol{\omega}_{bi} \\ \dot{\boldsymbol{\omega}}_{bi} &= -\boldsymbol{J}_{\mathrm{s}}^{-1}\boldsymbol{\omega}_{bi}^{\times}\boldsymbol{J}_{\mathrm{s}}\boldsymbol{\omega}_{bi} + \boldsymbol{J}_{\mathrm{s}}^{-1}(\boldsymbol{u}+\boldsymbol{d}) \end{aligned} \tag{14}$$

Denote $\boldsymbol{F}(\boldsymbol{e})=(\boldsymbol{t}^b)^{\times}=\begin{bmatrix} 0 & -e_z & e_y \\ e_z & 0 & -1-e_x \\ -e_y & 1+e_x & 0 \end{bmatrix}$. Then

$$\boldsymbol{F}(\boldsymbol{e})^{\mathrm{T}}\boldsymbol{e} = [\,0\ e_z\ -e_y\,]^{\mathrm{T}} = \begin{bmatrix} 0 & 0 & 0 \\ 0 & 0 & 1 \\ 0 & -1 & 0 \end{bmatrix}\boldsymbol{e} = \boldsymbol{P}\boldsymbol{e} \tag{15}$$

4. CONTROL STRUCTURE FOR REPOINTING MANEUVER

The repointing error dynamics in (14) can be expressed as an affine nonlinear system

$$\dot{\boldsymbol{x}} = \boldsymbol{f}(\boldsymbol{x}) + \boldsymbol{g}(\boldsymbol{x})(\boldsymbol{u}+\boldsymbol{d}) \tag{16}$$

where $\boldsymbol{x} = \begin{bmatrix} \boldsymbol{e} \\ \boldsymbol{\omega}_{bi} \end{bmatrix}$, $\boldsymbol{f}(\boldsymbol{x}) = \begin{bmatrix} \boldsymbol{F}\boldsymbol{\omega}_{bi} \\ \boldsymbol{J}_{\mathrm{s}}^{-1}\boldsymbol{\omega}_{bi}^{\times}\boldsymbol{J}_{\mathrm{s}}\boldsymbol{\omega}_{bi} \end{bmatrix}$, $\boldsymbol{g} = \begin{bmatrix} \boldsymbol{0}_{3\times 3} \\ \boldsymbol{J}_{\mathrm{s}}^{-1} \end{bmatrix}$.

The control objective for space target observation is to design a control law $\boldsymbol{u}$ so that the state in (16) can converge to zero while minimizing the performance index

$$J = \int_0^{\infty} (l(\boldsymbol{x}) + \boldsymbol{u}^{\mathrm{T}}\boldsymbol{R}\boldsymbol{u})dt \tag{17}$$

with $l(\boldsymbol{x}) = \boldsymbol{x}^{\mathrm{T}}\boldsymbol{Q}\boldsymbol{x}$.

For the repointing error dynamics (16), to combine the terminal sliding mode theory with the CLF approach, a proper Lyapunov function V should be constructed to make $L_gV = \boldsymbol{s}$ where $\boldsymbol{s}$ is a terminal sliding mode surface. Define V as follows:

$$\begin{aligned} V = &\begin{bmatrix} \boldsymbol{\xi}_1{}^{\mathrm{T}} & \boldsymbol{\omega}_e^{\mathrm{T}} \end{bmatrix} \begin{bmatrix} \frac{a_1}{2}\mathbf{I} & \frac{\alpha_1}{2}\boldsymbol{J}_{\mathrm{s}}(2+e_x) \\ \frac{\alpha_1}{2}J_s(2+e_x) & \frac{c}{4}J_s \end{bmatrix} \begin{bmatrix} \boldsymbol{\xi}_1 \\ \boldsymbol{\omega}_e \end{bmatrix} \\ &+ \begin{bmatrix} \boldsymbol{\xi}_2{}^{\mathrm{T}} & \boldsymbol{\omega}_e^{\mathrm{T}} \end{bmatrix} \begin{bmatrix} \frac{a_2}{2}I & \frac{\alpha_2}{2}\boldsymbol{J}_{\mathrm{s}}(2+e_x) \\ \frac{\alpha_2}{2}\boldsymbol{J}_{\mathrm{s}}(2+e_x) & \frac{c}{4}\boldsymbol{J}_{\mathrm{s}} \end{bmatrix} \begin{bmatrix} \boldsymbol{\xi}_2 \\ \boldsymbol{\omega}_e \end{bmatrix} \end{aligned} \tag{18}$$

which is positive definite if $\frac{a_1 c}{8}\boldsymbol{J}_{\mathrm{s}} > \frac{\alpha_1^2}{4}\boldsymbol{J}_{\mathrm{s}}^2(2+e_x)^2$, $\frac{a_2 c}{8}\boldsymbol{J}_{\mathrm{s}} > \frac{\alpha_2^2}{4}\boldsymbol{J}_{\mathrm{s}}^2(2+e_x)^2$ with $\boldsymbol{\xi}_1 = \mathbf{sig}(\boldsymbol{P}\boldsymbol{e})^{p_1/r_1}$, $\boldsymbol{\xi}_2 = \mathbf{sig}(\boldsymbol{P}\boldsymbol{e})^{m_1/n_1}$, $a_1 > 0$, $a_2 > 0$, $\alpha_1 > 0$, $\alpha_2 > 0$, $c > 0$. The symbol of $\mathbf{sig}(\boldsymbol{x})^a$ is a compact expression for the vector $\mathbf{sig}(\boldsymbol{x})^a = [|x_1|^a\mathrm{sign}(x_1), |x_2|^a\mathrm{sign}(x_2), ..., |x_n|^a\mathrm{sign}(x_n)]^{\mathrm{T}}$.

To avoid the singularity when calculating the equivalent control law, a modification for $\boldsymbol{s}$, called 'switching sliding mode surface technique' is adopted where the modified sliding surface $\boldsymbol{s}$ comprises two parts(see Lu and Xia (2013); Jiang et al. (2016)):

$$\begin{aligned} &\boldsymbol{s} = c\boldsymbol{\omega}_e + \boldsymbol{s}_e \\ &\boldsymbol{s}_e = \begin{cases} (2+e_x)(\alpha_1\mathbf{sig}(\boldsymbol{P}\boldsymbol{e})^{p_1/r_1} + \alpha_2\mathbf{sig}(\boldsymbol{P}\boldsymbol{e})^{m_1/n_1}), \\ \text{if } \min(|e_y|, |e_z|) > \varepsilon \\ l_1(2+e_x)\boldsymbol{P}\boldsymbol{e} + l_2(2+e_x)\mathbf{sig}(Pe)^{\alpha_3},\ \text{else} \end{cases} \end{aligned} \tag{19}$$

where $1 < \alpha_3 < 2$, $p_1 < r_1 < 2p_1$, $m_1 > n_1$. Note that in the existed literatures (Zuo and Tie (2014)), α_3 is always selected to be 2. However, there is no need to make $\alpha_3 = 2$ since $1 < \alpha_3$ is enough to ensure the nonsingularity. l_1 and l_2 should be calculated as follows to guarantee the continuity of the $\boldsymbol{s}_e$ and $\dot{\boldsymbol{s}}_e$, namely make $\boldsymbol{s}_e(\varepsilon^+) = \boldsymbol{s}_e(\varepsilon^-)$, $\dot{\boldsymbol{s}}_e(\varepsilon^+) = \dot{\boldsymbol{s}}_e(\varepsilon^-)$. Based on the segmented nonsingular terminal sliding mode surface, the two-phase TSCLF control scheme for repointing maneuver is designed as

$$\begin{aligned} &\boldsymbol{u} = \begin{cases} \boldsymbol{u}_1{}^*, & \text{if } \|L_gV\| \geq \delta \\ \boldsymbol{u}_2{}^*, & \text{else} \end{cases}, \\ &\boldsymbol{u}_1{}^* = -\boldsymbol{R}^{-1}\left[\frac{a + \sqrt{a^2 + l(\boldsymbol{x})\boldsymbol{b}\boldsymbol{R}^{-1}\boldsymbol{b}^{\mathrm{T}}}}{\boldsymbol{b}\boldsymbol{R}^{-1}\boldsymbol{b}^{\mathrm{T}}}\right]\boldsymbol{b}^{\mathrm{T}} \\ &\boldsymbol{u}_2{}^* = \boldsymbol{\omega}_{bi}^{\times}\boldsymbol{J}_{\mathrm{s}}\boldsymbol{\omega}_{bi} - \frac{1}{c}\boldsymbol{J}_{\mathrm{s}}\dot{\boldsymbol{s}}_e - \frac{k_1}{c}\boldsymbol{J}_{\mathrm{s}}\mathbf{sig}(\boldsymbol{s})^{p_2/r_2} \\ &\qquad -\frac{k_2}{c}\boldsymbol{J}_{\mathrm{s}}\mathbf{sig}(\boldsymbol{s})^{m_2/n_2} \end{aligned} \tag{20}$$

Theorem 1. For the attitude repointing system (16) with limited disturbance $\boldsymbol{d}(\|\boldsymbol{d}\| \leq \bar{d})$, if the states enter the area of Ω_1 at time T_s under the suboptimal CLF control law $\boldsymbol{u}_1^*$, the following conclusions are derived.

1) The sliding mode variable $\boldsymbol{s}$ defined in (19) would stay in Ω_1 and converge to the region $\Omega_s \subset \Omega_1$in finite time $T < T_s + T_1$ regardless of the initial states under the control law $\boldsymbol{u}_2^*$. Ω_1, Ω_s and T_1 are expressed as follows:

$$\Omega_1 = \{\boldsymbol{s} \,|\|\boldsymbol{s}\| < \delta\} \tag{21}$$

$$\Omega_s = \left\{\boldsymbol{s} \,\middle|\, k_1\theta_{p1}\|\boldsymbol{s}\| + k_2 \cdot 3^{\frac{n_2-m_2}{2n_2}}\theta_{g1}\|\boldsymbol{s}\|^{m_2/n_2} < \bar{d}\right\} \tag{22}$$

$$T_1 \leq \frac{r_2}{k_1(1-\theta_{p1})(r_2-p_2)} + \frac{n_2}{k_2 \cdot 3^{\frac{n_2-m_2}{2n_2}}(1-\theta_{g1})} \tag{23}$$

2) The repointing error $\boldsymbol{e}$ can converge to the neighborhood Ω_{e1} of equilibrium in finite time $T < T_s + T_1 + T_2$ or to Ω_{e2} in finite time $T < T_\varepsilon + T_2^{'}$ where T_ε is the time for $\min(|e_y|, |e_z|) = \varepsilon$. The expressions for Ω_{e1}, Ω_{e2}, T_2 and $T_2^{'}$ is shown as follows.

$$\Omega_{e1} = \left\{ \|\boldsymbol{Pe}\| \,\middle|\, \frac{\alpha_1}{c}\delta_x(1+\delta_x)\theta_{p_2}\|\boldsymbol{Pe}\|^{p_1/r_1} + 2^{\frac{n_1-m_1}{2n_1}}\frac{\alpha_2}{c}\delta_x(1+\delta_x)\theta_{g_2}\|\boldsymbol{Pe}\|^{m_1/n_1} < \frac{\Delta_s}{c} \right\} \tag{24}$$

$$T_2 \leq \frac{1}{\frac{\alpha_1}{c}2^{\frac{p_1+r_1}{2r_1}}\delta_x(1+\delta_x)(1-\theta_{p2})(\frac{r_1-p_1}{2r_1})} + \frac{1}{\frac{2\alpha_2}{c}\delta_x(1+\delta_x)(1-\theta_{g2})(\frac{m_1-n_1}{2n_1})} \tag{25}$$

$$\Omega_{e2} = \left\{ \boldsymbol{e} \,\middle|\, \|\boldsymbol{Pe}\| \leq \frac{\Delta_s}{l_1\delta_x(1+\delta_x)\theta_{p_3}} = \Delta_{e2} \right\} \tag{26}$$

$$T_2^{'} \leq \frac{\ln(V_e(t=T_\varepsilon)) - \ln(\Delta_{V_e})}{\frac{2}{c}l_1\delta_x(1+\delta_x)(1-\theta_{p3})} \tag{27}$$

Proof.

Step 1. Assume that the state enters into the region of Ω_1 at time T_s under the suboptimal CLF control law $\boldsymbol{u}_1^*$, then to show the convergence of the sliding mode variable $\boldsymbol{s}$ defined in (19), construct the following Lyapunov function

$$V_s = \boldsymbol{s}^{\mathrm{T}}\boldsymbol{s} \tag{28}$$

The derivative of V_s with the terminal sliding mode control law $\boldsymbol{u}_2^*$ in (20) is

$$\begin{aligned}\dot{V}_s &= 2\boldsymbol{s}^{\mathrm{T}}\left[c\boldsymbol{J}_{\mathrm{s}}{}^{-1}(-\boldsymbol{\omega}_{bi}^{\times}\boldsymbol{J}_{\mathrm{s}}\boldsymbol{\omega}_{bi} + \boldsymbol{u}_2^* + \boldsymbol{d}) + \dot{\boldsymbol{s}}_e\right] \\ &= -2k_1\boldsymbol{s}^{\mathrm{T}}\mathbf{sig}(\boldsymbol{s})^{\frac{p_2}{r_2}} - 2k_2\boldsymbol{s}^{\mathrm{T}}\mathbf{sig}(\boldsymbol{s})^{\frac{m_2}{n_2}} + 2\boldsymbol{s}^{\mathrm{T}}\boldsymbol{d} \\ &\leq -2k_1 V_s{}^{\frac{p_2+r_2}{2r_2}} - 2k_2 \cdot 3^{\frac{n_2-m_2}{2n_2}} V_s{}^{\frac{n_2+m_2}{2n_2}} + 2\bar{d}V_s{}^{1/2}\end{aligned} \tag{29}$$

From (29) we can get that $\boldsymbol{s}$ could converge to the area of Ω_s from Ω_1 in finite time T_1 where Ω_s and T_1 is obtained based on the fixed-time control theory as shown in (22) and (23).

Denote the switch time as T_s at which the control switch from $\boldsymbol{u}_1^*$ to $\boldsymbol{u}_2^*$. When $t > T_s + T_1$, according to the convergence region of $\boldsymbol{s}$ given in (22), the norm of $\boldsymbol{s}$ is limited within

$$\|\boldsymbol{s}\| < \Delta_s = \min\left\{ \left[\frac{\bar{d}}{k_1(1-\theta_{p1})}\right]^{\frac{r_2}{p_2}}, \left[\frac{\bar{d}}{k_2 \cdot 3^{\frac{n_2-m_2}{2n_2}}\theta_{g1}}\right]^{\frac{n_2}{m_2}} \right\}$$

where θ_{p1} and θ_{g1} are positive constants satisfying $\theta_{p1}, \theta_{g1} \in (0,1)$.

Step 2. Suppose that the sliding variable $\boldsymbol{s}$ converges to the value of $\boldsymbol{s} = \boldsymbol{s}_{\Delta 1}, \|\boldsymbol{s}_{\Delta 1}\| < \Delta_s$ when $t > T_s + T_1$. Next the convergence of the repointing error $\boldsymbol{e}$ will be analyzed. Since the sliding mode surface in (19) contains two segments to avoid singularity, the convergence property of the system should be dicussed seperately by using the segmented sliding mode control law in (20).

Case 1: $\min(|e_y|, |e_z|) > \varepsilon$ for $t > T_s + T_1$.

Considering the residual of $\boldsymbol{s}$, the sliding mode surface in (19) can be written as

$c\boldsymbol{\omega}_e = -(2+e_x)[\alpha_1\mathbf{sig}(\boldsymbol{Pe})^{\frac{p_1}{r_1}} + \alpha_2\mathbf{sig}(\boldsymbol{Pe})^{\frac{m_1}{n_1}}] + \boldsymbol{s}_{\Delta 1}$

Construct a novel Lyapunov function composed of the repointing errors

$$V_e = \frac{1}{2}(e_y^2 + e_z^2) = \frac{1}{2}(\boldsymbol{Pe})^{\mathrm{T}}(\boldsymbol{Pe}) \tag{30}$$

Then differentiating V_e with respect to time along the system function (16) yields that

$$\begin{aligned}\dot{V}_e \leq\ & -(1+e_x)(2+e_x)\left[\frac{\alpha_1}{c}2^{\frac{p_1+r_1}{2r_1}}V_e{}^{\frac{p_1+r_1}{2r_1}} + \frac{2\alpha_2}{c}V_e{}^{\frac{m_1+n_1}{2n_1}}\right] \\ & + \frac{\sqrt{2}}{c}|1+e_x|\,\|V_e\|\,\Delta_s\end{aligned} \tag{31}$$

Assume that $1 + e_x = \cos\theta_x > \delta_x \geq 0$ when $t > T_s + T_1$, where δ_x is a constant. This assumption implies that the angle between the target direction and the optical axis X_b is smaller than $\pi/2$ when $t > T_s + T_1$ which is rational in practice. Then, the (31) is modified as

$$\begin{aligned}\dot{V}_e \leq\ & -\frac{\alpha_1}{c}2^{\frac{p_1+r_1}{2r_1}}\delta_x(1+\delta_x)V_e{}^{\frac{p_1+r_1}{2r_1}} \\ & -\frac{2\alpha_2}{c}\delta_x(1+\delta_x)V_e{}^{\frac{m_1+n_1}{2n_1}} + \frac{\sqrt{2}}{c}V_e{}^{0.5}\Delta_s\end{aligned} \tag{32}$$

Thus V_e can converge to the region of Ω_{e1} in (24) after $t > T_s + T_1 + T_2$

where T_2 is given in (25). $\theta_{p2}, \theta_{g2} \in (0,1)$ are positive constants. In light of (24), it can be derived that when $t > T_s + T_1 + T_2$,

$$\|\boldsymbol{Pe}\| < \Delta_{e1} = \min\left\{ \left(\frac{\Delta_s}{\alpha_1\delta_x(1+\delta_x)\theta_{p_2}}\right)^{\frac{r_1}{p_1}}, \left(\frac{\Delta_s 2^{\frac{m_1-n_1}{2n_1}}}{\alpha_2\delta_x(1+\delta_x)\theta_{g_2}}\right)^{\frac{n_1}{m_1}} \right\} \tag{33}$$

Case 2: $\min(|e_y|, |e_z|) \leq \varepsilon$ for $t > T_\varepsilon > T_s + T_1$, where T_ε is the time when $\min(|e_y|, |e_z|) = \varepsilon$.

In this case, the sliding mode surface in (19) is changed to the second segment as

$$c\boldsymbol{\omega}_e = -l_1(2+e_x)\boldsymbol{Pe} - l_2(2+e_x)\mathbf{sig}(\boldsymbol{Pe})^{\alpha_3} + \boldsymbol{s}_{\Delta 1} \tag{34}$$

Likewise, the Lyapunov function and its derivative can be formulated as

$$V_e = \frac{1}{2}(e_y^2 + e_z^2) = \frac{1}{2}(\boldsymbol{Pe})^{\mathrm{T}}(\boldsymbol{Pe}) \tag{35}$$

$$\begin{aligned}\dot{V}_e &= (1+e_x)(\boldsymbol{Pe})^{\mathrm{T}}\boldsymbol{\omega}_e \leq -\frac{2l_1}{c}\delta_x(1+\delta_x)V_e + \frac{\sqrt{2}}{c}V_e{}^{0.5}\Delta_s \\ &= -\frac{2l_1}{c}(1-\theta_{p_3})\delta_x(1+\delta_x)V_e \\ &\quad -\frac{2l_1}{c}\theta_{p_3}\delta_x(1+\delta_x)V_e + \frac{\sqrt{2}}{c}V_e{}^{0.5}\Delta_s\end{aligned} \tag{36}$$

which implies that the repointing error $\boldsymbol{e}$ can reach and stay in the region of Ω_{e2} after $t = T_\varepsilon + T_2^{'}$.

$\theta_{p_3} \in (0,1)$ is a positive constant. $T_2^{'}$ is the convergence time of which the state converge from $\boldsymbol{e}_{t=T_\varepsilon}$ to Ω_{e2}. When the state is out of the set of Ω_{e2},

$$\dot{V}_e \leq -\frac{2l_1}{c}(1-\theta_{p_3})\delta_x(1+\delta_x)V_e \tag{37}$$

Integrating both sides of (37) yields the convergence time $T_2^{'}$ in (27).

To sum up, the final convergence region of the repointing error $\boldsymbol{e}$ hinges upon the value of Δ_{e1} and ε: If $\Delta_{e1} \leq \sqrt{2}\varepsilon$, then $\lim_{t\to T_\varepsilon+T_2^{'}} \boldsymbol{e} \to \Omega_{e2}$, else the convergence region can not be definitely decided. The convergence time for different cases are summarized in Table 1.

Table 1. Convergence time and region for different cases

	$\Delta_{e1} \leq \sqrt{2}\varepsilon$	$\Delta_{e1} > \sqrt{2}\varepsilon$	
Convergence time	$T_s + T_1 + T_2$	$T_s + T_1 + T_2$	$T_\varepsilon + T_2^{'}$
Convergence region	Ω_{e1}	Ω_{e1}	Ω_{e2}

5. NUMERICAL SIMULATIONS

The moment of inertia of the spacecraft is chosen to be $\boldsymbol{J}_s = \text{diag}[86.24, 85.07, 113.59]$, the unit space target direction $\boldsymbol{t}^b = [2\ 1\ 1]^{\mathrm{T}}/\sqrt{6}$, the controller parameters in (20) are selected to be $a_1 = 1.53$, $a_2 = 1.9$, $\alpha_1 = 0.05$, $\alpha_2 = 0.05$, $c = 1.2$, $k_1 = 1$, $k_2 = 1$, $p_1 = 9$, $r_1 = 11$, $m_1 = 7$, $n_1 = 5$, $p_2 = 7$, $r_2 = 9$, $m_2 = 9$, $n_2 = 7$, $\alpha_3 = 1.5$, $\delta = 5.3 \times 10^{-3}$. External disturbances are $\boldsymbol{d}(t)$= $0.1 \times [\sin(0.1t),\ -\cos(0.1t),\ \sin(0.1t)]^{\mathrm{T}}$ (N · m).

The simulation results are illustrated in Fig. 1-Fig. 4. To show the superiority of the TSCLF over the classical CLF method(CCLF), the comparison is conducted. As can be seen from Fig.1 which shows the angles between the target direction and three body-fixed axis, $\theta_x \approx 0.02°$ in the end for TSCLF approach. While, for the classical CLF method, the control precision is so bad that the repointing error is 2°.

For TSCLF, the control law switches from CLF control to sliding mode control at $t = 6$s when the state is near the sliding mode surface $\boldsymbol{s}$. The phase plot of the states trajectories and the sliding mode surface is shown in Fig. 3, where s_3 is one of the components of $\boldsymbol{s}$ designed in (19).

To verify the optimality of the TSCLF control scheme with respect to the performance index given in (17), the trajectories of the cost-to-go function both for TSCLF, CCLF and the real optimal control are given in Fig. 4. The accumulated cost of TSCLF, namely the integral of (17) is 31.35 which is a little more than the real optimal results (29.4) obtained by using the optimization software. While CCLF accumulates a cost of 30.4.

Although the TSCLF consumes more energy than CCLF, the difference is too little to be of concern. The control precision and performance index by using CCLF and TSCLF for different target observations are listed in Table 2. In general, TSCLF performs better than CCLF in terms of control precision and stability.

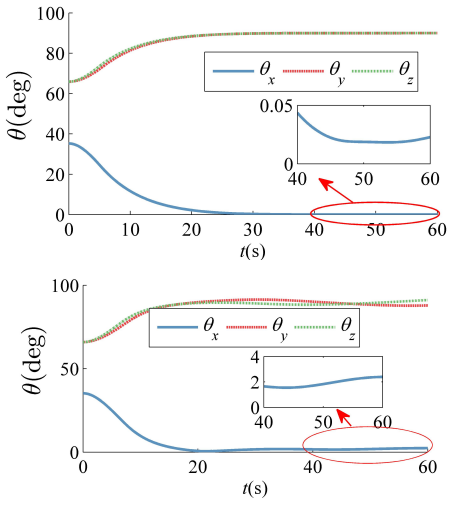

Fig. 1. Angles between the target orientation and three body axes for space target observation

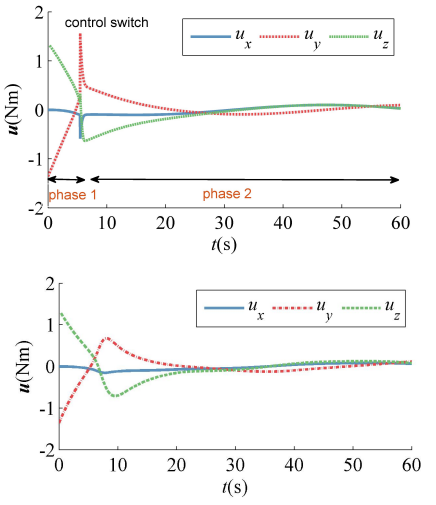

Fig. 2. Control torque histories for space target observation by using different controllers

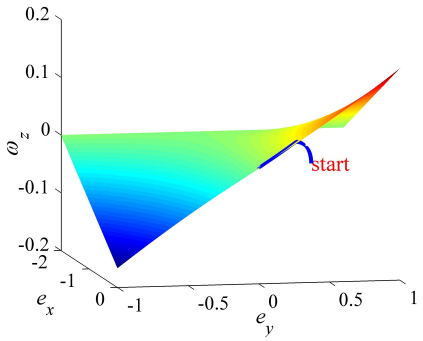

Fig. 3. Sliding mode surface of s_3 for space target observation

6. CONCLUSION

A new way to define the repointing error kinematics is presented, which is convenient for optimal controller design and analysis. An improved CLF control scheme called the two-phase CLF (TSCLF) is presented combining fixed-

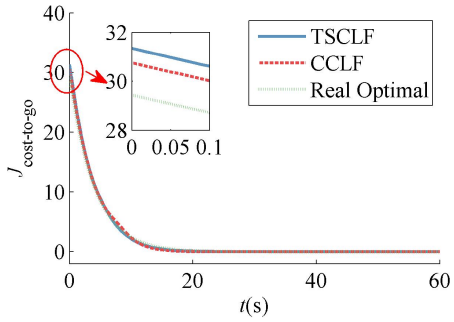

Fig. 4. Cost to go functions of different control schemes for space target observation

Table 2. Performance comparisons between TSCLF and CCLF for different space target directions

Target direction	Pointing error(∘)		Performance index	
	TSCLF	CCLF	TSCLF	CCLF
$[2,1,1]$	0.022	2.364	32.9	32.5
$[2,3,1]$	0.023	2.345	86.4	86.65
$[2,7,1]$	0.023	2.327	137.7	222.5
$[1,-2,1]$	0.023	2.327	105.93	105.3
$[-1,3,4]$	0.022	2.33	238.7	240.9
$[-1,1,1]$	0.028	2.31	499.4	1254.2
$[1,4,2]$	0.023	2.337	145.4	144.9

time sliding mode control theory with a CLF. This control is able to optimally drive the state to the sliding surface and then converge to a neighborhood of the origin along this surface in a fixed-time. This control enables this fixed-time to be prescribed independently of initial conditions. Compared with the classical CLF approach, the TSCLF method not only guarantees the optimality of the system but also improves the robustness to disturbances.

ACKNOWLEDGEMENTS

This work is supported by China Scholarship Council, the National Natural Science Foundation of China (Grants No. 61876050, 61973100 and 61673135).

REFERENCES

Lian Y, Gao Y, Zeng G. Staring imaging attitude control of small satellites. Journal of Guidance, Control, and Dynamics, 2017, 40(5): 1278-1285.

Pong C M, Miller D W. Reduced-attitude boresight guidance and control on spacecraft for pointing, tracking, and searching. Journal of Guidance, Control, and Dynamics, 2015, 38(6): 1027-1035.

Geng Y, Li C, Guo Y, et al. Fixed-time near-optimal control for repointing maneuvers of a spacecraft with nonlinear terminal constraints. ISA transactions, 2020, 97: 401-414.

Park Y. Robust and optimal attitude stabilization of spacecraft with external disturbances. Aerospace Science and Technology, 2005, 9(3): 253-259.

Haddad W M, L'Afflitto A. Finite-time stabilization and optimal feedback control. IEEE Transactions on Automatic Control, 2015, 61(4): 1069-1074.

Primbs J A, Nevistić V, Doyle J C. Nonlinear optimal control: A control Lyapunov function and receding horizon perspective. Asian Journal of Control, 1999, 1(1): 14-24.

Corradini M L, Cristofaro A. Nonsingular terminal sliding-mode control of nonlinear planar systems with global fixed-time stability guarantees. Automatica, 2018, 95: 561-565.

Zuo Z. Non-singular fixed-time terminal sliding mode control of non-linear systems. IET control theory & applications, 2014, 9(4): 545-552.

Zuo Z. Nonsingular fixed-time consensus tracking for second-order multi-agent networks. Automatica, 2015, 54: 305-309.

Wang L, Chai T, Zhai L. Neural-network-based terminal sliding-mode control of robotic manipulators including actuator dynamics. IEEE Transactions on Industrial Electronics, 2009, 56(9): 3296-3304.

Sontag E D. A 'universal' construction of Artstein's theorem on nonlinear stabilization. Systems & control letters, 1989, 13(2): 117-123.

Zuo Z, Tie L. A new class of finite-time nonlinear consensus protocols for multi-agent systems. International Journal of Control, 2014, 87(2): 363-370.

Lu K, Xia Y. Adaptive attitude tracking control for rigid spacecraft with finite-time convergence. Automatica, 2013, 49(12): 3591-3599.

Jiang B, Hu Q, Friswell M I. Fixed-time attitude control for rigid spacecraft with actuator saturation and faults. IEEE Transactions on Control Systems Technology, 2016, 24(5): 1892-1898.

Hu Q, Chi B, Akella M R. Anti-Unwinding Attitude Control of Spacecraft with Forbidden Pointing Constraints. Journal of Guidance, Control, and Dynamics, 2018, 42(4): 822-835.

Hu Q, Jiang B, Zhang Y. Observer-based output feedback attitude stabilization for spacecraft with finite-time convergence. IEEE Transactions on Control Systems Technology, 2017, 27(2): 781-789.

Hu Q, Shao X, Chen W H. Robust fault-tolerant tracking control for spacecraft proximity operations using time-varying sliding mode. IEEE Transactions on Aerospace and Electronic Systems, 2017, 54(1): 2-17.

Hu Q, Chen W, Guo L. Fixed-Time Maneuver Control of Spacecraft Autonomous Rendezvous With a Free-Tumbling Target. IEEE Transactions on Aerospace and Electronic Systems, 2018, 55(2): 562-577.